



# Wüstite stability in the presence of a CO<sub>2</sub>-fluid and a carbonate-silicate melt: Implications for the graphite/diamond formation and generation of Fe-rich mantle metasomatic agents



Yuliya V. Bataleva <sup>a,b,\*</sup>, Yuri N. Palyanov <sup>a,b</sup>, Alexander G. Sokol <sup>a,b</sup>, Yuri M. Borzdov <sup>a,b</sup>, Oleg A. Bayukov <sup>c</sup>

<sup>a</sup> Sobolev Institute of Geology and Mineralogy, Siberian Branch of Russian Academy of Sciences, Koptyug ave 3, Novosibirsk 630090, Russia

<sup>b</sup> Novosibirsk State University, Pirogova str 2, Novosibirsk 630090, Russia

<sup>c</sup> Kirensky Institute of Physics, Siberian Branch of Russian Academy of Sciences, Akademgorodok 50, bld. 38, Krasnoyarsk 660036, Russia

## ARTICLE INFO

### Article history:

Received 10 July 2015

Accepted 3 December 2015

Available online 12 December 2015

### Keywords:

Wüstite  
CO<sub>2</sub>-fluid  
Carbonate-silicate melt  
Decarbonation  
Graphite formation  
HPHT experiment

## ABSTRACT

Experimental simulation of the interaction of wüstite with a CO<sub>2</sub>-rich fluid and a carbonate-silicate melt was performed using a multianvil high-pressure split-sphere apparatus in the FeO-MgO-CaO-SiO<sub>2</sub>-Al<sub>2</sub>O<sub>3</sub>-CO<sub>2</sub> system at a pressure of 6.3 GPa and temperatures in the range of 1150 °C–1650 °C and with run time of 20 h. At relatively low temperatures, decarbonation reactions occur in the system to form iron-rich garnet (Alm<sub>75</sub>Prp<sub>17</sub>GrS<sub>8</sub>), magnesiowüstite (Mg# ≤ 0.13), and CO<sub>2</sub>-rich fluid. Under these conditions, magnesiowüstite was found to be capable of partial reducing CO<sub>2</sub> to C<sup>0</sup> that leads to the formation of Fe<sup>3+</sup>-bearing magnesiowüstite, crystallization of magnetite and metastable graphite, and initial growth of diamond seeds. At T ≥ 1450 °C, an iron-rich carbonate-silicate melt (FeO ~ 56 wt.%, SiO<sub>2</sub> ~ 12 wt.%) forms in the system. Interaction between (Fe,Mg)O, SiO<sub>2</sub>, fluid and melt leads to oxidation of magnesiowüstite and crystallization of fayalite-magnetite spinel solid solution (1450 °C) as well as to complete dissolution of magnesiowüstite in the carbonate-silicate melt (1550 °C–1650 °C). In the presence of both carbonate-silicate melt and CO<sub>2</sub>-rich fluid, dissolution (oxidation) of diamond and metastable graphite was found to occur. The study results demonstrate that under pressures of the lithospheric mantle in the presence of a CO<sub>2</sub>-rich fluid, wüstite/magnesiowüstite is stable only at relatively low temperatures when it is in the absolute excess relative to CO<sub>2</sub>-rich fluid. In this case, the redox reactions, which produce metastable graphite and diamond with concomitant partial oxidation of wüstite to magnetite, occur. Wüstite is unstable under high concentrations of a CO<sub>2</sub>-rich fluid as well as in the presence of a carbonate-silicate melt: it is either completely oxidized or dissolves in the melt or fluid phase, leading to the formation of Fe<sup>2+</sup>- and Fe<sup>3+</sup>-enriched carbonate-silicate melts, which are potential metasomatic agents in the lithospheric mantle.

© 2015 Elsevier B.V. All rights reserved.

## 1. Introduction

Ferropericlase is believed to be the most abundant oxide mineral in the Earth's interior, e.g., (Mg,Fe)O is thought to account for about 20 vol.% of the lower mantle (Dubrovinsky et al., 2000; Fei et al., 1992; Kaminsky, 2012; Lin et al., 2003; Mao et al., 1996; Ringwood, 1991). Studies of inclusions in natural diamonds from kimberlite pipes in Brazil, Guinea, and Canada demonstrate that oxides of Fe and Mg can amount to ~50% of all inclusions (Harte, 2010; Harte et al., 1999; Kaminsky, 2012; McCammon, 2001; McCammon et al., 2004; Wirth et al., 2014). X<sub>Fe</sub> (Fe/(Fe + Mg) ratio) of ferropericlase inclusions in lower-mantle diamonds is 0.10–0.65 (Harte and Hudson, 2013; Harte et al., 1999; Hayman et al., 2005; Kaminsky, 2012; McCammon et al.,

1997; Svicer, 1995; Wirth et al., 2014), while magnesiowüstite with X<sub>Fe</sub> from ≥0.5 to pure wüstite is typical of the upper mantle assemblages (Bulanova, 1995; Stachel et al., 1998; Svicer, 1995). The highest ferric iron content (Fe<sup>3+</sup>/ΣFe) of all (Mg,Fe)O crystals found in diamonds is ~0.07 (McCammon et al., 1997). The mechanism of concentration and incorporation of ferric iron in ferropericlase and magnesiowüstite affects the iron transport (atomic diffusion, electrical conductivity) and rheological properties (Mackwell et al., 2005; Tremper et al., 1974; Wood and Nell, 1991).

Variations in the P–T–fO<sub>2</sub> conditions and chemical composition of a host mantle domain cause changes in the ferric iron concentration in (Mg,Fe)O by orders of magnitude (Kaminsky et al., 2015; McCammon et al., 1997; McCammon et al., 2004; Otsuka et al., 2010, 2013) and can strongly affect the phase relations and element partitioning between (Mg,Fe)O and coexisting minerals or melts (Frost and McCammon, 2008; Rohrbach and Schmidt, 2011). The formation of oxidized mantle regions with a high oxygen fugacity, which is reflected

\* Corresponding author at: Koptyug ave 3, Novosibirsk 630090, Russia. Tel./fax: +7 3832 330 75 01.

E-mail address: [bataleva@igm.nsc.ru](mailto:bataleva@igm.nsc.ru) (Y.V. Bataleva).

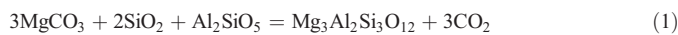
in the Fe<sup>3+</sup>-bearing magnesiowüstite formation and supported by the presence of carbonate minerals (Biellmann et al., 1993; Boulard et al., 2011; Brenker et al., 2007; Kaminsky et al., 2013; Stagno et al., 2011), is usually associated with subduction (Kaminsky et al., 2015; McCammon et al., 2004). The input of subducted material may lead not only to an overall increase in *f*O<sub>2</sub> in local mantle domains but also enable the redox reactions involving magnesiowüstite and oxidized phases of the down-going slab, such as carbonates, CO<sub>2</sub>, or carbonatitic melts, e.g., according to the following simplified schemes: 4FeO + CO<sub>2</sub> → 2Fe<sub>2</sub>O<sub>3</sub> + C<sup>0</sup> (Boulard et al., 2011) and 6FeO + CO<sub>2</sub> → 2Fe<sub>3</sub>O<sub>4</sub> + C<sup>0</sup> (Zhang et al., 1999).

Although minerals of the MgO–FeO series are thermodynamically stable over a very wide range of pressures and temperatures, most of the modern experimental studies are devoted to investigating ferropericlase properties under the conditions of the lower mantle, while the number of studies on the behavior of magnesiowüstite in the upper mantle is still small. A study (Mao et al., 1996) emphasizes the “enigmatic” and “paradoxal” features of wüstite (in contrast to periclase) that emerged from extensive studies of oxidation-reduction, disproportionation, and metallization of FeO. Here, we present the results of experimental simulation of the redox interaction of wüstite/magnesiowüstite with a CO<sub>2</sub>-rich fluid and a carbonate-silicate melt that are implicated in the graphite and diamond formation and estimation of the wüstite stability in the presence of CO<sub>2</sub>-bearing fluids and melts and the generation of Fe-rich mantle metasomatic agents.

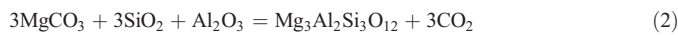
## 2. Methods

### 2.1. Starting materials

A carbonate–oxide mixture, undergoing decarbonation under experimental *P–T* conditions, was used as a source of CO<sub>2</sub>-rich fluid. Previous experimental studies in the carbonate-silicate systems (Knoche et al., 1999; Pal'yanov et al., 2005) have demonstrated that the largest amount of a CO<sub>2</sub>-rich fluid in decarbonation reactions is released during the garnet formation (compared to reactions of pyroxene and olivine crystallization):



(Knoche et al., 1999)



(Pal'yanov et al., 2005)

According to gas chromatography data, in the MgCO<sub>3</sub>–SiO<sub>2</sub>–Al<sub>2</sub>O<sub>3</sub> system at *P* = 6.0 GPa, *T* = 1600 °C, *t* = 40 h (experiments using Pt capsules) composition of fluid, formed via decarbonation, was about 93 mol.% CO<sub>2</sub>, 6 mol.% H<sub>2</sub>O and 1 mol.% CH<sub>4</sub> + H<sub>2</sub> (Pal'yanov et al., 2005). Thus, a mixture of MgCO<sub>3</sub>, SiO<sub>2</sub>, and Al<sub>2</sub>O<sub>3</sub> can be used as a reliable source for CO<sub>2</sub>-rich fluid.

The starting materials consisted of synthetic SiO<sub>2</sub> and Al<sub>2</sub>O<sub>3</sub> (99.99% purity), natural magnesite (MgCO<sub>3</sub>), and dolomite (CaMg(CO<sub>3</sub>)<sub>2</sub>) (Chelyabinsk Region, Russia) (Table 1). Dolomite was introduced in the system as a source of calcium and to initiate decarbonation reaction at relatively low temperatures. Starting magnesite and dolomite were used at an 8:1 molar ratio (bulk carbonate composition, Mg<sub>0.9</sub>Ca<sub>0.1</sub>CO<sub>3</sub>).

**Table 1**

Composition of initial carbonates and bulk composition of the FeO–MgO–CaO–SiO<sub>2</sub>–Al<sub>2</sub>O<sub>3</sub>–CO<sub>2</sub> system.

Mass concentration (wt.%)	Si	Al	Fe	Mg	Mn	Ca	C	O	Total
Magnesite	–	–	0.3	28.1	0.2	–	14.3	57.1	100
Dolomite	–	–	0.3	12.8	0.2	21.5	13	52.2	100
Bulk system	10	6.4	28.2	7.7	–	1.3	4.2	42.2	100

The proportions of carbonates, SiO<sub>2</sub>, and Al<sub>2</sub>O<sub>3</sub> were selected so that the (Mg + Ca):Al:Si molar ratio was 3:2:4. The complete reaction of these carbonates and oxides under experimental *P–T* conditions leads to the formation of a CO<sub>2</sub>-rich fluid and also to crystallization of garnet (pyrope), with a small excess of SiO<sub>2</sub> (Pal'yanov et al., 2005).

To simulate the composition of wüstite, which is unstable under atmospheric conditions, a mixture of metallic iron and Fe<sub>2</sub>O<sub>3</sub> (99.99% purity), in molar proportion 1:1, was used. A special experiment at *P* = 6.3 GPa, *T* = 1150 °C, *t* = 18 h demonstrated that the initial mixture of Fe<sup>0</sup> and Fe<sub>2</sub>O<sub>3</sub> completely reacts at 1150 °C to form coarse-crystalline wüstite:



Quantities of the starting materials were as follows: 114 mg of MgCO<sub>3</sub>, 28 mg of CaMg(CO<sub>3</sub>)<sub>2</sub>, 56.8 mg of Al<sub>2</sub>O<sub>3</sub>, 101.2 mg of SiO<sub>2</sub>, 43 mg of Fe<sup>0</sup>, and 129 mg of Fe<sub>2</sub>O<sub>3</sub>. A composition of initial carbonates and bulk composition of the system are presented in Table 1.

### 2.2. High-pressure experiments

The experiments were conducted on a multianvil high-pressure split-sphere apparatus (BARS) at pressure of 6.3 GPa, in the temperature range of 1150 °C–1650 °C, and with run time of 20 h. A high-pressure cell in the form of tetragonal prism, 21.1 × 21.1 × 25.4 mm in size, was used. The elongated cell geometry enabled using graphite heaters of 12 mm in diameter and 18.8 mm in length. The temperature was measured in each experiment by a PtRh<sub>30</sub>/PtRh<sub>6</sub> thermocouple. Details on the pressure and temperature calibration were presented elsewhere (Pal'yanov et al., 2002a, 2002b; Palyanov et al., 2010).

The methodical approach and corresponding scheme of the reaction ampoule assembly were developed in (Palyanov et al., 2007), and their efficiency for studying interactions in the carbonate–oxide and carbonate systems involving mantle minerals-concentrators of iron was demonstrated in several studies (Bataleva et al., 2012a, b, 2015; Palyanov et al., 2013). Application of this approach provides conditions for decarbonation reactions, interaction of the formed silicates and CO<sub>2</sub>-rich fluid with iron-rich phases as well as for the generation of ferric and ferrous carbonate-silicate melts under mantle *P–T* conditions. It should be especially noted that similar “sandwich”-type schemes of experimental charge are developed and used to study reaction zoning of samples, not to study equilibrium conditions. An initial scheme of a reaction ampoule is shown in Fig. 1. A mixture of Al<sub>2</sub>O<sub>3</sub>, SiO<sub>2</sub>, MgCO<sub>3</sub>, and CaMg(CO<sub>3</sub>)<sub>2</sub> (total weight of 300 mg) was placed into the Pt capsule with a diameter of 10 mm. A pellet (*d* = 5 mm, 150 mg) of Fe<sup>0</sup> and Fe<sub>2</sub>O<sub>3</sub> (wüstite-simulating mixture) was put inside a carbonate–oxide mixture. Therefore, the phases-concentrators of iron were separated from the Pt-capsule by the carbonate–oxide ampoule with an external diameter of 9.5 mm and a wall thickness of 2.2 mm. Synthetic diamond seed crystals of the cuboctahedral shape, 0.5 mm in size, were placed in the carbonate–oxide ampoule (Fig. 1), to enable evaluating whether the redox conditions in the reaction ampoules correspond to the stability

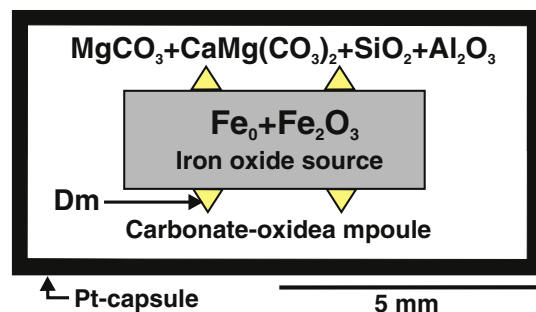


**Fig. 1.** Scheme of the initial ampoule assembly. Dm, diamond seed crystal.

field of free carbon. The filled ampoules were sealed by arc welding. The sealed capsule height varied from 3.5 to 4.0 mm. One of the main advantages of the methodical approach used is the possibility to use Pt capsules when working with Fe-rich phases at high  $P$ – $T$  parameters. Pt is known to be the optimal material for high-pressure high-temperature experiments involving fluids and melts. However, it is not appropriate for Fe-bearing systems when the traditional procedure of grinding and homogenization of starting materials is used. Insulation of an iron-concentrator from the Pt capsule by a carbonate–oxide sleeve allows for studies involving iron-rich phases and for preservation of tightness in the reaction volume, while the iron–platinum interaction is minimized. Analysis of the Pt-capsule material after experiments demonstrated that the concentration of Fe in Pt is less than 0.2 wt.% at  $T \leq 1350$  °C and is about 1.0–1.2 wt.% in the range of 1450 °C–1650 °C, which is also confirmed by the mass balance calculations. The presence of fluid bubbles in samples (Fig. 2) is further evidence of Pt capsule tightness.

### 2.3. Analytical procedures

Phase identification of all samples was made using X-ray diffraction (DRON-3 X-ray diffractometer with  $\text{CuK}\alpha$  radiation). XRD patterns were registered in the  $2\theta$  range of  $10^\circ$ – $70^\circ$ . Interpretation of XRD patterns was performed using the ASTM database. Chemical compositions of the products of experiments were studied by microprobe analysis (Camebax-Micro analyzer) and energy-dispersive spectroscopy (Tescan MIRA3 LMU scanning electron microscope). For the microprobe and EDS analyses, samples in the form of polished sections were prepared. For all the analyses of silicate and oxide crystalline phases, an accelerating voltage of 20 kV, a probe current of 20 nA, counting time of 20 s, and beam diameter of 2–4  $\mu\text{m}$  were used. For carbonates and quenched melt, the accelerating voltage was lowered to 15 kV, probe current was lowered to 10 nA, counting time was lowered to 10 s, and a defocused beam ( $d = 20$ – $100$   $\mu\text{m}$ ) was used. Standards for the analyses of melt phase were natural pyrope, almandine, enstatite, diopside, kyanite, and magnesite. Mass balance calculations (the least-squares method) were performed only for experiments at  $T \geq 1450$  °C (Table 2) because, at lower temperatures, the compositions of final phases varied in a rather wide range. These calculations were performed for a restricted number of components of the system, namely, MgO, CaO,  $\text{SiO}_2$ , and  $\text{Al}_2\text{O}_3$ . We excluded FeO,  $\text{Fe}_2\text{O}_3$ , and  $\text{CO}_2$  from the calculations because of uncertainties in their concentrations according to microprobe and iron migration to Pt. Investigation of the phase relationships was conducted by scanning electron microscopy using the Tescan MIRA3 LMU scanning electron microscope. Methodologically complex problems of studying the  $\text{Fe}^{2+}$  and  $\text{Fe}^{3+}$  distribution patterns in the resulting phase assemblages as well as the  $\text{Fe}^{2+}/\text{Fe}^{3+}$  ratio calculation were solved using Mössbauer spectroscopy. Mössbauer measurements were

performed at room temperature on a MC-1104Em spectrometer equipped with a  $\text{Co}^{57}(\text{Cr})$  source using powder absorbers with a thickness of 1–5  $\text{mg}/\text{cm}^2$ . The spectrum acquisition time for each sample was 80 h. Detailed procedure of the identification of the spectra is presented in the Supplementary Materials section.

## 3. Results

### 3.1. Experimental results on the interaction between wüstite and $\text{CO}_2$ -rich fluid at 6.3 GPa and in the temperature range of 1150 °C–1350 °C

The experimental results are presented in Table 2 and Fig. 3. At relatively low temperatures (1150 °C–1250 °C), coarse crystalline magnesiowüstite is formed in the central part of the samples (Figs. 3a, 4a). At the contact between the carbonate–oxide ampoule and magnesiowüstite, a reaction zone is formed that consists predominantly of garnet as well as metastable graphite and magnetite (Figs. 3a, 4a,b), while the peripheral part of the ampoule is represented predominantly by ferromagnesite, coesite, and corundum. The formation of garnet in the reaction zone indicates the occurrence of decarbonation processes during the carbonate–oxide interaction, even in a relatively low temperature range. It should be noted that the garnet produced at 1150 °C and 1250 °C is characterized by ferromagnesite inclusions (Fig. 4c) and magnetite reaction rims around single garnet crystals or garnet aggregates. The reaction zone width at the contact of the carbonate–oxide ampoule with magnesiowüstite broadens as experimental temperatures are increased, whereas the amount of coarse crystalline magnesiowüstite in the central part of the ampoules decreases. The initial stage of diamond growth was observed on diamond seed crystals in the temperature range of 1150 °C–1250 °C. At 1350 °C, magnetite is found not only in the reaction zone but also in the central part of the ampoule in the assemblage with magnesiowüstite. In this case, the assemblage of garnet + magnesiowüstite + magnetite + orthopyroxene + ferromagnesite + metastable graphite forms at the place of the carbonate–oxide ampoule.

Compositions of the resulting phases based on microprobe analysis are shown in Table 3. In the temperature range of 1150 °C–1250 °C, magnesiowüstite is a predominant oxide in samples, but the quantity of magnetite increases with temperature, and at 1350 °C, the quantity of magnetite exceeds that of magnesiowüstite. Magnetite was found to be always in the association with garnet and metastable graphite (Fig. 4a, b) that are formed in the reaction zone. The composition of the resulting magnesiowüstite varies from  $\text{Fe}_{0.99}\text{Mg}_{0.01}\text{O}$  (1150 °C) to  $\text{Fe}_{0.87}\text{Mg}_{0.13}\text{O}$  (1350 °C), i.e. a regular increase in Mg# with the temperature occurs. According to the results of the Mössbauer spectroscopy, wüstite is found to be characterized by a large number of cation vacancies as well as relatively high values of  $\text{Fe}^{3+}/(\text{Fe}^{2+} + \text{Fe}^{3+}) \sim 0.05$ – $0.12$  ( $\pm 0.03$ ) that increase as the experimental temperature is increased (Table 4, Fig. 5a). The magnetite composition almost completely

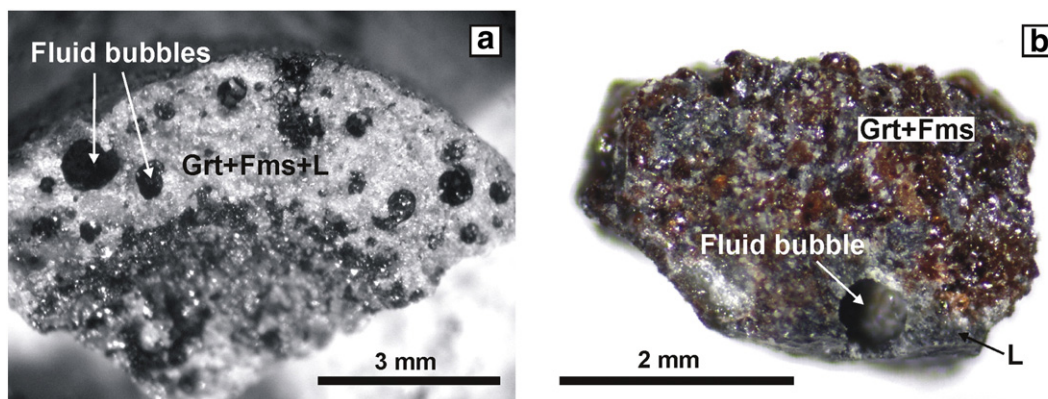
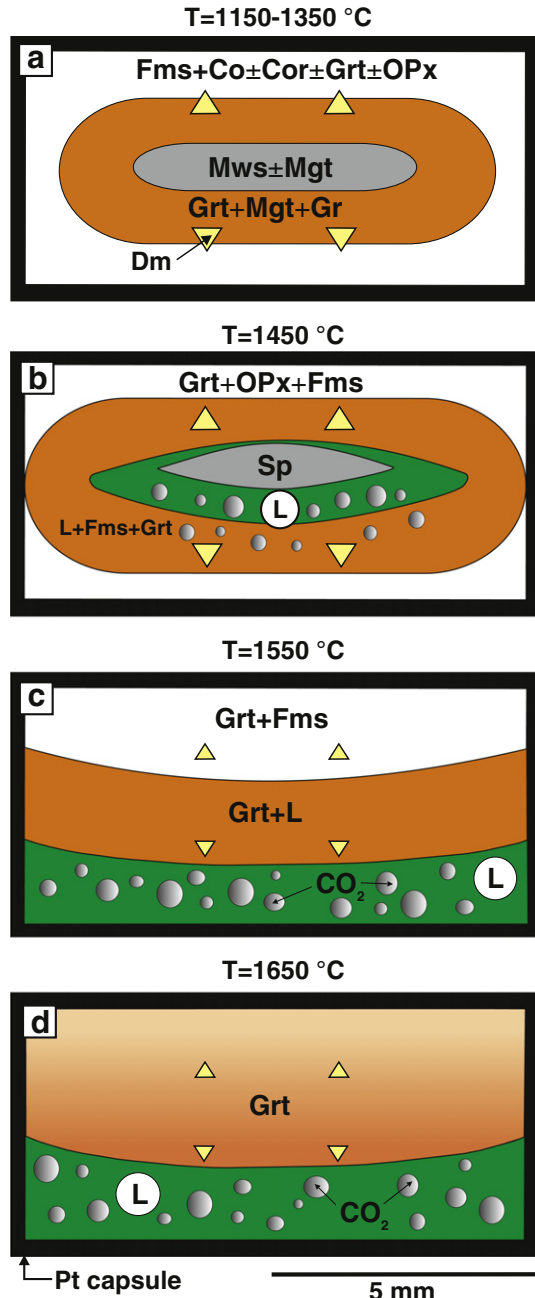


Fig. 2. Optical micrographs of the samples: a,  $\text{CO}_2$ -rich fluid bubbles, with walls covered by graphite films, in the polycrystalline garnet-ferromagnesite aggregate (1450 °C); b,  $\text{CO}_2$ -rich fluid bubble in the quenched carbonate-silicate melt (1550 °C); Grt, pyrope-almandine; Fms, ferromagnesite; L, carbonate-silicate melt; fluid bubbles, segregated  $\text{CO}_2$ -rich fluid.

**Table 2**Results of the experiments in FeO–MgO–CaO–SiO<sub>2</sub>–Al<sub>2</sub>O<sub>3</sub>–CO<sub>2</sub> system at  $P = 6.3$  GPa,  $T = 1150$  °C–1650 °C and duration of 20 h.

Run no.	$T$ (°C)	Silicates, oxides, carbonates	Carbon phases	Carbonate-silicate melt	Weight proportions of phases (wt.%) <sup>*</sup>				
					Grt	Fms	Sp	Melt	CO <sub>2</sub>
1289	1150	Mws + Mgt + Grt + OPx + Fms + Co + Cor	Gr, DG	–					
1287	1250	Mws + Mgt + Grt + OPx + Fms	Gr, DG	–					
1283	1350	Mws + Mgt + Grt + OPx + Fms	Gr, DD	–					
1359	1450	Grt + Fms + Sp	Gr, DD	+	40	16	6	36	2
1284	1550	Grt + Fms	DD	+	48	24	–	26	2
1242	1650	Grt	DD	+	46	–	–	51	4

Notes: <sup>\*</sup>, weight proportions of final phases were calculated from mass balance; Grt, garnet; Fms, ferromagnesite; OPx, orthopyroxene; Mws, magnesiowüstite; Mgt, magnetite; Sp, fayalite-magnetite spinel solid solution; Co, coesite; Cor, corundum; Gr, metastable graphite; DG, diamond growth on seeds; DD, diamond dissolution.



**Fig. 3.** Schemes of carbonate–oxide interaction: a, 1150 °C–1350 °C; b, 1450 °C; c, 1550 °C; d, 1650 °C. Grt, garnet (pyrope–almandine); OPx, orthopyroxene (ferrosilite); Fms, ferromagnesite; Mws, magnesiowüstite; Mgt, magnetite; Co, coesite; Cor, corundum; Dm, diamond seed crystals; Sp, spinel of magnetite–fayalite composition; L, carbonate–oxide melt; Gr, metastable graphite; CO<sub>2</sub>, fluid bubbles.

corresponds to the stoichiometric composition, except the SiO<sub>2</sub> impurity of about 1.3–1.5 wt.%, which is typical of magnetite from the mantle rock xenoliths and diamond inclusions (Prinz et al., 1975; Sobolev et al., 1998; Stachel et al., 1998).

As it was shown before, in the range of 1150 °C–1250 °C, the formation of garnet occurs mainly in the reaction zone, at the contact with magnesiowüstite. In the reaction zone, garnet associated with magnetite and metastable graphite compositionally belongs to pyrope–almandine, with composition of Alm<sub>75</sub>Prp<sub>17</sub>Gr<sub>8</sub> (1150 °C) and Alm<sub>46</sub>Prp<sub>39</sub>Gr<sub>15</sub> (1350 °C). According to the data of microprobe analysis, garnet is characterized by cation sums, exceeding 8, and total Fe p.f.u higher than 2.62 (Table 3). Calculations using the method of Finger (1972) showed that garnet formed at 1150 °C–1350 °C can bear up to 7 wt.% of Fe<sub>2</sub>O<sub>3</sub>. With increasing experimental temperature and a corresponding increase in the decarbonation degree of the system, the FeO content in garnet is significantly decreased (Table 3; Fig. 6). Ferromagnesite is one of the main products of the interaction in the system at relatively low temperatures. The ferromagnesite composition tends to decrease in the Fe content and correspondingly increase in Mg# (Table 3) as the temperature is increased and varies from Fe<sub>0.66</sub>Mg<sub>0.31</sub>Ca<sub>0.02</sub>CO<sub>3</sub> (1150 °C) to Fe<sub>0.58</sub>Mg<sub>0.40</sub>Ca<sub>0.03</sub>CO<sub>3</sub> (1350 °C). The CaO content in ferromagnesite is very low, about 0.5–1.5 wt.%, and temperature-independent.

### 3.2. Experimental results on the interaction between wüstite, CO<sub>2</sub>-rich fluid and carbonate-silicate melt at 6.3 GPa and in the temperature range of 1450 °C–1650 °C

A scheme of the sample from the experiment at 1450 °C is shown at Fig. 3b. It has been established that the products of this experiment lack magnesiowüstite and magnetite, and a central part of the sample contains only coarse crystalline spinel—a solid solution of fayalite and magnetite (this mantle phase was described by Woodland and Angel (2000)). A peripheral part of the reaction ampoule consists of a polycrystalline aggregate of garnet and ferromagnesite that comprises spherical cavities, which are formed most probably by a segregated CO<sub>2</sub>-rich fluid (Fig. 2a). The cavity walls are covered with a graphite film. At this temperature, a formation of the first portions of a carbonate-silicate melt is found, which are mostly located around the fayalite-magnetite spinel (Fig. 3b) and in the interstices of a polycrystalline aggregate of garnet and ferromagnesite (Fig. 4d). According to data from energy-dispersive spectroscopy, a dendritic aggregate of fayalite-magnetite spinel, ferrosilite, and ferromagnesite forms from the melt during quenching (Fig. 4d). Identification of the Mössbauer spectra obtained for a bulk sample from the experiment at 1450 °C revealed that the association of iron-bearing phases in the sample is represented by siderite, almandine, and spinel in a 51:31:18 ratio (Fig. 5b; Supplementary Table 1; Supplementary Fig. 1). The main phases-concentrators of Fe<sup>2+</sup> are siderite and almandine; Fe<sup>3+</sup> and Fe<sup>4+</sup> were detected in the spinel composition (Fig. 5b).

At temperatures higher than 1450 °C, phases, coexisting with fluid and melt, are represented by garnet and ferromagnesite and form the so-called carbonate-silicate matrix. In the presence of the melt and

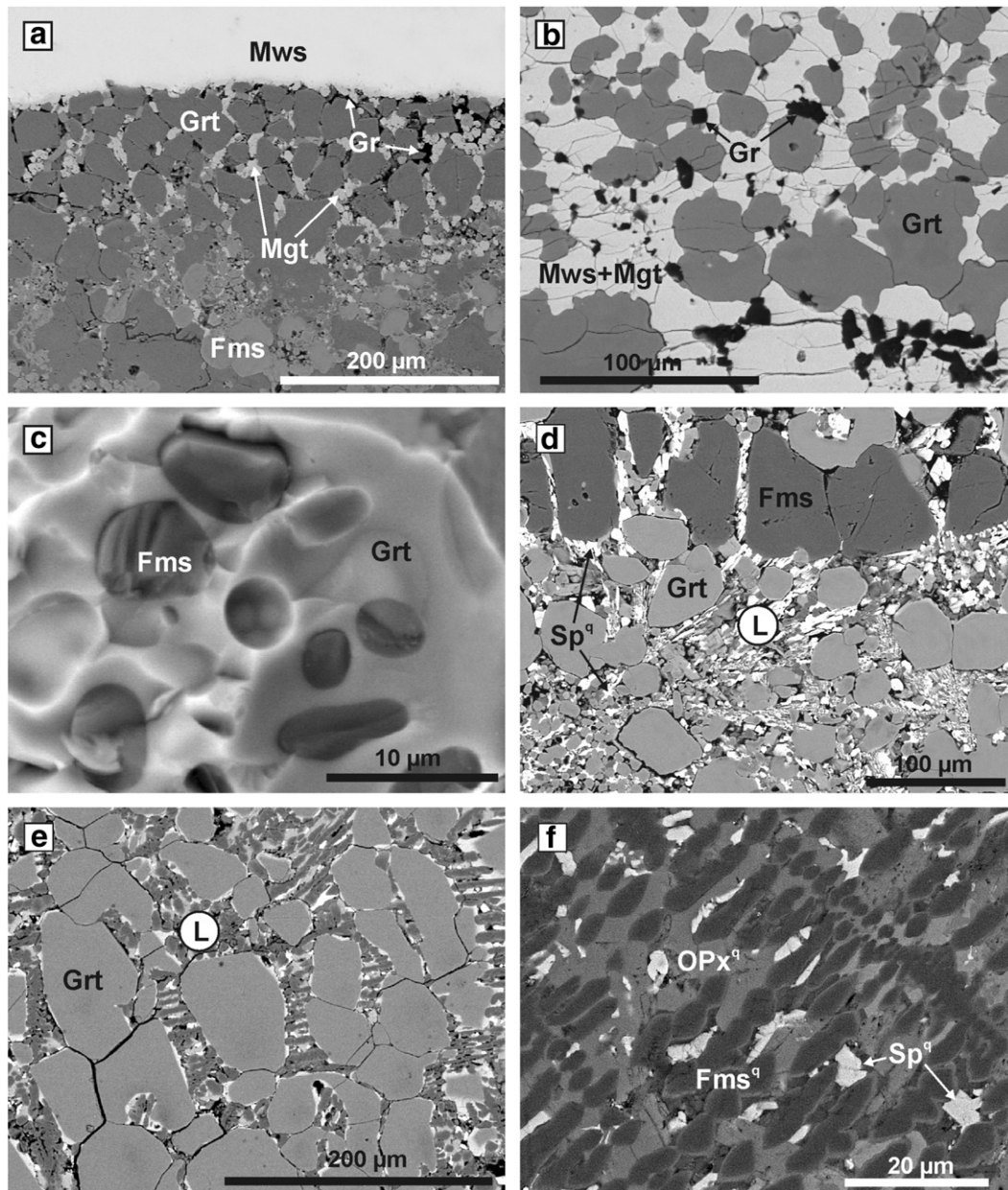


**Fig. 4.** SEM-micrographs (a,b,d–f, polished sections; c, cleaved surface): a, reaction zone, consisting of almandine, metastable graphite, and magnetite at the contact with magnesiowustite (1150 °C); b, polycrystalline aggregate of magnesiowustite, magnetite, pyrope-almandine, and metastable graphite from reaction zone (1250 °C); c, inclusions of ferromagnesite in pyrope-almandine from reaction zone (1250 °C); d, pyrope-almandine and ferromagnesite crystals in dendritic aggregate (i.e. quenched melt) (spinel + orthopyroxene + ferromagnesite), central part of the sample (1450 °C); e, pyrope-almandine in dendritic aggregate (orthopyroxene + ferromagnesite + spinel), central part of the sample (1550 °C); f, structure of quenched melt, lower part of the sample (1550 °C); Grt, garnet (pyrope-almandine); OPx<sup>q</sup>, orthopyroxene (ferrosilite); Fms, ferromagnesite; Mws, magnesiowustite; Mgt, magnetite; Gr, metastable graphite; Sp, spinel of magnetite-fayalite composition; L, carbonate-oxide melt; <sup>q</sup>, quenched phases.

segregated fluid, significant dissolution of diamond seed crystals occurs, and samples lack graphite. At 1550 °C, the resulting phases are garnet, ferromagnesite, a carbonate-silicate melt (Figs. 3c, 4e,f), and a CO<sub>2</sub>-rich fluid, which forms cavities of up to 1.2 mm in size (Fig. 2b). At 1650 °C, the formation of garnet, a CO<sub>2</sub>-rich fluid, and a carbonate-silicate melt was observed (Fig. 3d).

Assessments of the melting degrees and the results of the mass balance calculations for relatively high-temperature experiments are shown in Table 2, compositions of final phases are presented in Table 3. The fayalite-magnetite spinel solid solution is characterized by the composition of ~Fa<sub>80</sub>Mgt<sub>20</sub>. Garnet composition varies from Alm<sub>24</sub>Prp<sub>64</sub>GrS<sub>12</sub> (1450 °C) to Alm<sub>47</sub>Prp<sub>50</sub>GrS<sub>3</sub> (1650 °C). The iron-rich garnet produced by decarbonation of the system is characterized by the main tendency of the FeO content to decrease as the temperature

is increased (Fig. 6), with the exception of the experiment at 1450 °C, where garnet crystallization is accompanied by the formation of the first portion of an iron-rich carbonate-silicate melt, and therefore, the concentration of FeO in pyrope-almandine is significantly reduced. In addition to the high Fe content, the characteristic feature of the resulting garnet is relatively low concentrations of MgO, which increase with temperature, as well as the almost constant CaO content (Table 3). Composition of ferromagnesite, which is stable up to  $T = 1550$  °C, varies from Fe<sub>0.53</sub>Mg<sub>0.47</sub>Ca<sub>0.01</sub>CO<sub>3</sub> (1450 °C) to Fe<sub>0.43</sub>Mg<sub>0.55</sub>Ca<sub>0.02</sub>CO<sub>3</sub> (1550 °C). Using Mössbauer spectroscopy, it was established that at temperatures of 1550 °C and 1650 °C, iron in garnet as well as in ferromagnesite occurs only in the ferrous state.

The first portions of a carbonate-silicate melt generated at 1450 °C are characterized by extremely high concentrations of ΣFe, amounting

**Table 3**

Averaged compositions of mineral phases and melts.

Run no.	T (°C)	Phase	N <sub>A</sub>	Mass concentration (wt.%)				Cations per formula unit								
				SiO <sub>2</sub>	Al <sub>2</sub> O <sub>3</sub>	FeO*	MgO	CaO	Total	Si	Al	Fe	Mg	Ca	C**	Total
1289	1150	Grt	17	37.1 (12)	16.8 (11)	38.5 (21)	4.8 (19)	3.4 (3)	100.5	3.03	1.62	2.62	0.59	0.3	–	8.15 <sup>a</sup>
		Fms	15	–	–	45.3 (18)	11.9 (20)	1.3 (1)	58.5	–	–	0.67	0.32	0.03	0.99	2
		Mws	12	–	–	99.3 (1)	0.6 (1)	–	99.9	–	–	0.99	0.01	–	–	1
		Mgt	13	1.3 (1)	–	91.5 (7)	0.3 (1)	–	93.2	0.05	–	2.88	0.02	–	–	2.95
1287	1250	Grt	18	36.9 (13)	18.2 (11)	35.3 (19)	5.7 (20)	3.7 (3)	99.8	2.99	1.74	2.39	0.69	0.32	–	8.14 <sup>a</sup>
		OPx	7	47.7 (6)	–	47.5 (9)	4.4 (8)	1.1 (1)	100.7	2.01	–	1.66	0.28	0.05	–	3.99
		Fms	11	–	–	40.6 (15)	13.3 (16)	2.2 (2)	56.1	–	–	0.58	0.34	0.04	1.02	1.98
		Mgt	10	1.4 (1)	–	92.8 (6)	0.9 (1)	–	95.1	0.05	–	2.85	0.05	–	–	2.95
1283	1350	Mws	13	–	–	93.9 (10)	6.9 (11)	–	100.9	–	–	0.88	0.12	–	–	1
		Grt	14	38.9 (14)	21.4 (17)	22.8 (16)	10.6 (19)	5.6 (8)	99.4	2.98	1.93	1.46	1.22	0.46	–	8.05 <sup>a</sup>
		OPx	8	47.6 (3)	0.3 (1)	38.9 (10)	11.9 (6)	0.5 (1)	99.3	1.95	0.01	1.33	0.73	0.02	–	4.04
		Fms	14	–	–	40.5 (21)	15.5 (18)	1.4 (2)	57.4	–	–	0.58	0.4	0.03	0.99	2
1359	1450	Mws	10	–	–	91.7 (13)	7.5 (14)	–	99.2	–	–	0.87	0.13	–	–	1
		Mgt	10	1.4 (1)	0.2 (1)	93.2 (02)	1.4 (0.1)	–	96.3	0.05	0.01	2.82	0.08	–	–	2.96
		Grt	12	42.5 (15)	23.2 (1.0)	11.9 (1)	18.1 (1.5)	4.7 (0.3)	100.4	3.04	1.95	0.71	1.94	0.36	–	7.99
		Fms	14	–	–	37.5 (20)	18.7 (1.8)	0.8 (0.1)	56.9	–	–	0.53	0.47	0.01	0.99	2.01
1284	1550	Sp	11	21.2 (1)	–	71.9 (2)	–	–	93.1	0.83	–	2.34	–	–	–	3.17 <sup>a</sup>
		L	26	12.0 (15)	0.9 (2)	56.0 (24)	6.1 (1.8)	1.5 (7)	76.4	–	–	–	–	–	–	–
		Grt	17	39.8 (9)	21.2 (8)	24.1 (4)	9.6 (5)	5.4 (1)	100.2	3.04	1.9	1.53	1.1	0.44	–	8.01
		Fms	17	–	–	31.4 (2)	23.1 (1)	1.6 (2)	56.1	–	–	0.43	0.57	0.03	0.99	2.02
1242	1650	L	23	13.7 (25)	2.6 (21)	35.9 (11)	9.2 (17)	8.7 (12)	70.0	–	–	–	–	–	–	–
		Grt	23	39.9 (11)	22.3 (20)	23.8 (19)	14.0 (18)	1.3 (4)	101.0	2.97	1.95	1.48	1.56	0.1	–	8.05
		L	31	8.8 (20)	5.1 (3)	38.0 (10)	15.4 (4)	4.2 (4)	71.5	–	–	–	–	–	–	–
		L	31	8.8 (20)	5.1 (3)	38.0 (10)	15.4 (4)	4.2 (4)	71.5	–	–	–	–	–	–	–

Grt, garnet; OPx, orthopyroxene; Fms, ferromagnesite; Mws, magnesiowüstite; Mgt, magnetite; Sp, magnetite-fayalite spinel solid solution; L, carbonate-silicate melt; FeO\*, total FeO + Fe<sub>2</sub>O<sub>3</sub>; C\*\*, calculated from a sum deficit; N<sub>A</sub>, the number of electron probe analyses used to obtain the average compositions. The values in parentheses are one sigma errors of the means based on replicate electron microprobe analyses reported as least units cited; 37.1(12) should be read as 37.1 ± 1.2 wt.%; <sup>a</sup>, high cation sums are a result of Fe<sup>3+</sup>-incorporation.

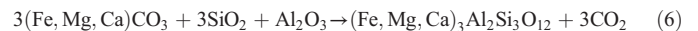
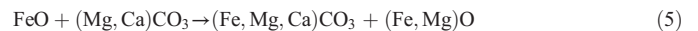
to 56 wt.% (Table 2), and also by the SiO<sub>2</sub> content of about 12 wt.%. A quench aggregate of the resulting melt consists of fayalite-magnetite spinel, ferromagnesite, and ferrosilite (Fig. 4d) at a 22:13:2 mass ratio. Mg# and Ca# of the resulting carbonate-silicate melt are very low and amount to 0.16 and 0.02, respectively, and the concentration of Al<sub>2</sub>O<sub>3</sub> is less than 0.9 wt.%. Phases, coexisting with a melt, are represented by almandine, ferromagnesite, and fayalite-magnetite spinel solid solution. A melt, formed at 1550 °C, coexisting with garnet and ferromagnesite, crystallizes at the quench stage as an aggregate of ferrosilite, ferromagnesite, and fayalite-magnetite spinel (12:11:3 mass ratio). The ΣFe concentration in the produced carbonate-silicate melt is greatly decreased relative to the first portion and amounts to 35–36 wt.%. The concentration of SiO<sub>2</sub> in the melt is about 14 wt.%. Mg# and Ca# of the produced melt are increased relative to the melt formed at 1450 °C and amount to 0.26 and 0.18, respectively. The carbonate-silicate melt under these conditions contains up to 24 wt.% of CO<sub>2</sub> (as a component). In addition, at T ≥ 1450 °C, quench aggregates

of the carbonate-silicate melts were found to contain cavities formed by a segregated CO<sub>2</sub>-rich fluid (Fig. 2a,b). At 1650 °C, the degree of partial melting of the system is 51 wt.%, with garnet being the only solid phase. A quench aggregate of the carbonate-silicate melt consists of ferromagnesite, garnet, and fayalite-magnetite spinel (18:10:3 mass ratio). Concentration of FeO in the resulting melt is 38 wt.%, and the SiO<sub>2</sub> content is 9 wt.%. According to the Mössbauer data, a Fe<sup>3+</sup>/ΣFe value in quench aggregates is of 0.03–0.06 (Fig. 5c; Supplementary Table 1). The main feature of the melt compared to low temperature ones is elevated MgO concentrations (15 wt.%).

## 4. Discussion

### 4.1. Reconstruction of the phase formation processes accompanying the wüstite + CO<sub>2</sub>-rich fluid or carbonate-silicate melt interaction

In the range of 1150 °C–1250 °C, crystallization of the association of magnesiowüstite, magnetite, metastable graphite, and Fe-rich garnet at the contact of wüstite with the external carbonate-oxide ampoule occurs via sequential reactions of Fe,Mg,Ca-carbonate formation (5), decarbonation to form Fe-rich garnet and CO<sub>2</sub> (6), and a further reaction of CO<sub>2</sub> with wüstite (magnesiowüstite) (7):



Direct evidence of the reactions (5) and (6) is ferromagnesite inclusions, which are typical of the garnet from relatively low-temperature experiments (Fig. 4c). The redox reaction (7) can be regarded as reduction of a CO<sub>2</sub>-rich fluid by wüstite to elemental carbon (graphite,

**Table 4**<sup>57</sup>Fe Mössbauer data for magnesiowüstite.

Run no.	T (°C)	Iron valence (coordination number)	IS (mm/s)	QS (mm/s)	W (mm/s)	A (%)
1289	1150	Fe <sup>2+</sup>	0.963	0.40	0.33	27
			0.889	0.62	0.41	31
			0.925	1.03	0.42	26
			1.139	0.39	0.21	11
			0.355	1.02	0.20	5
1287	1250	Fe <sup>2+</sup>	0.945	0.36	0.31	30
			0.901	0.63	0.34	23
			0.934	1.07	0.38	26
			1.113	0.38	0.23	14
			0.321	0.75	0.29	7
1283	1350	Fe <sup>2+</sup>	0.961	0.32	0.37	24
			0.973	0.64	0.37	21
			0.936	0.95	0.49	37
			1.091	0.33	0.23	6
			0.399	0.81	0.34	12

IS, isomer shift with reference to α-Fe (error ± 0.005); QS, quadrupole splitting (error ± 0.02); W, width of the absorption line (error ± 0.02); A, (area(Fe<sup>2+</sup>))/(area(Fe<sup>2+</sup>) + area(Fe<sup>3+</sup>)) × 100% or (area(Fe<sup>3+</sup>))/(area(Fe<sup>2+</sup>) + area(Fe<sup>3+</sup>)) × 100% (error ± 3).

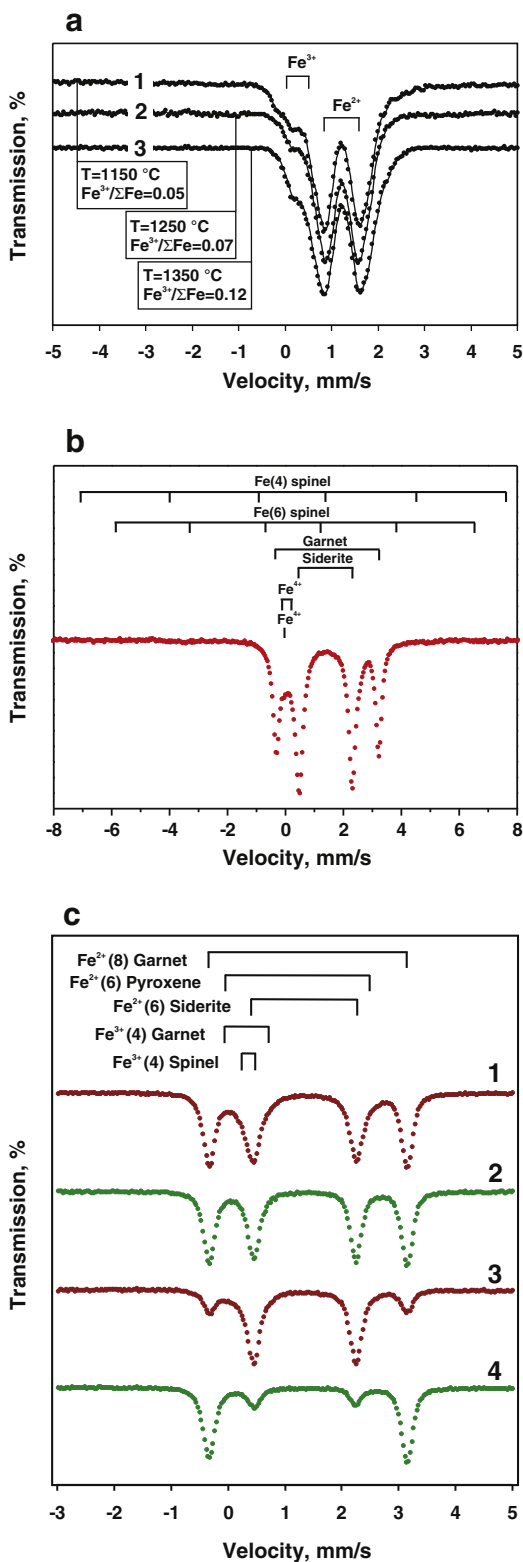


**Fig. 5.** Room-temperature Mössbauer spectra: a, magnesiowüstite from relatively low-temperature experiments (1150 °C–1350 °C); b, aggregate of garnet, siderite, and spinel crystals with interstitial quenched melt (1450 °C); c, 1, quenched carbonate-silicate melt with some garnet crystals (1550 °C); 2, garnet and siderite crystals (1550 °C); 3, quenched carbonate-silicate melt (1650 °C); 4, garnet polycrystalline aggregate with interstitial melt (1650 °C).

diamond) accompanied by oxidation of wüstite to magnetite. However, it should be noted that this reaction is possible only at relatively low temperatures, under conditions where FeO is in an absolute excess

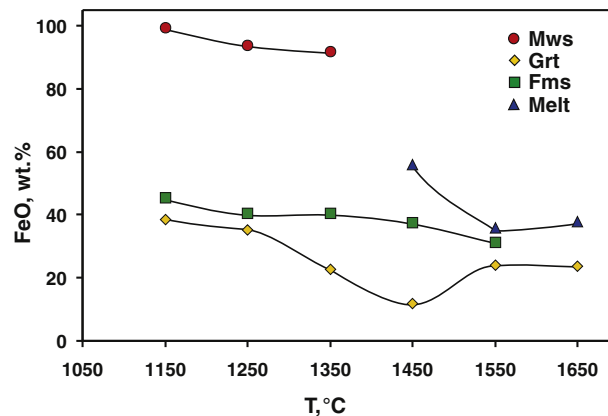
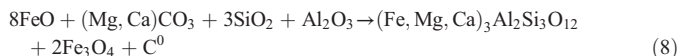
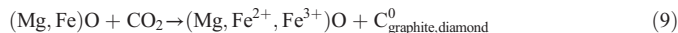


**Fig. 6.** Temperature dependence of FeO content in mineral phases and melts. Grt, garnet (pyrope-almandine); Fms, ferromagnesite; Mws, magnesiowüstite; Melt, carbonate-silicate melt.

relative to CO<sub>2</sub>. In summary, the following reaction (8) may be considered as the major one in the temperature range of 1150 °C–1250 °C:



According to the Mössbauer spectroscopy data, revealed ferric iron in the structure of magnesiowüstite, we can suggest that one of the reactions of reduction of CO<sub>2</sub> to C<sup>0</sup> to form metastable graphite and diamond at relatively low temperatures is the following redox reaction (shown schematically):



Thus, the assemblage of Fe<sup>3+</sup>-bearing magnesiowüstite and metastable graphite, and also an overgrown layer of diamond on seed crystals can be formed via reaction (9).

At higher temperatures (1350 °C–1450 °C), the degree of system decarbonation increases, and the garnet and CO<sub>2</sub>-rich fluid formation processes occur throughout the reaction volume. In this case, FeO is intensively consumed by garnet crystallization in reaction (6). A high degree of decarbonation of the system and an increase of the quantity of CO<sub>2</sub>-rich fluid results in strong oxidation of magnesiowüstite to magnetite via reactions (7) and (8). At 1350 °C, the amount of magnetite exceeds the amount of magnesiowüstite, and at 1450 °C, where first portion of carbonate-silicate melt is generated, interactions between (Fe,Mg)O, SiO<sub>2</sub>, fluid, and melt leads to the formation of fayalite-magnetite spinel solid solution. At 1450 °C, the degree of system decarbonation is very high, and segregated CO<sub>2</sub>-rich fluid forms CO<sub>2</sub> bubbles (Fig. 2a). During the formation of the carbonate-silicate melt (even though it forms in a small amount by volume), there is a sharp decrease in the iron concentration (Fig. 6) in garnet compared to both the subsolidus and higher temperature assemblages. At the highest temperatures (1550 °C–1650 °C), the main processes occurring in the system were found to be decarbonation, wüstite oxidation and partial melting as well as enrichment of the carbonate-silicate melt with FeO.

#### 4.2. Decarbonation parameters, formation of CO<sub>2</sub> and carbonate-silicate melt

The decarbonation processes play one of the main roles in the phase formation in the studied system. It was found that ferromagnesite is stable and only partly consumed by decarbonation in the range of 1150 °C–1550 °C, and reacts completely at higher temperatures. It should be noted that the parameters of partial and complete decarbonation of the studied system are in good agreement with the results

obtained in a study of partial melting in the (Mg,Ca)CO<sub>3</sub>-SiO<sub>2</sub>-Al<sub>2</sub>O<sub>3</sub>-(Mg,Fe)(Ti,Fe,Cr)O<sub>3</sub> system with similar *P* and *T* (Bataleva et al., 2012a). The interesting feature of the performed experiments is that the decarbonation reactions occur even at 1150 °C. According to the data of (Knoche et al., 1999), decarbonation with the formation of pure (Fe-free) pyrope at 6.3 GPa in the system MgCO<sub>3</sub>-SiO<sub>2</sub>-Al<sub>2</sub>SiO<sub>5</sub> cannot occur at temperatures below 1400 °C. Applying the results of calculations, performed by Berman (1991) for FeO-CaO-MgO-SiO<sub>2</sub>-Al<sub>2</sub>O<sub>3</sub>-CO<sub>2</sub> system, and experimental data (Knoche et al., 1999) for reconstruction of the decarbonation curve of the produced solid solution of Alm<sub>70</sub>Prp<sub>20</sub>Grs<sub>10</sub> garnet, we found that at 6.3 GPa decarbonation starts at about 1100 °C.

We have found the formation of fluid bubbles in a carbonate-silicate melt as well as in a carbonate-silicate matrix during studies of the carbonate-oxide (Bataleva et al., 2012a, b) and carbonate-oxide-sulfide (Palyanov et al., 2007) systems at a pressure of 6.3 GPa and in the range of 1550 °C–1700 °C. The emergence of a segregated fluid indicates not only a high degree of system decarbonation but also argues that the studied FeO-MgO-CaO-SiO<sub>2</sub>-Al<sub>2</sub>O<sub>3</sub>-CO<sub>2</sub> system does not reach the second critical point at pressure of 6.3 GPa.

Previous studies of the behavior of mantle minerals-concentrators of iron in the carbonate-oxide systems (Bataleva et al., 2012a, b, 2015; Palyanov et al., 2007) demonstrated that phases such as ilmenite, chromite, pyrrhotite, and metallic iron oxidize in the course of redox reactions with a CO<sub>2</sub>-rich fluid and carbonate-silicate melts in a wide temperature range at pressures of the lithospheric mantle. At the highest temperatures (*T* ≥ 1450 °C), one of the main products of the interaction in these systems is a carbonate-silicate melt and CO<sub>2</sub>-rich fluid in presence of which all the above listed mantle minerals, including wüstite, are unstable. The produced carbonate-silicate melts and CO<sub>2</sub>-rich fluids are potential agents of oxidative metasomatism of the mantle that are capable of dissolving and transporting large amounts of ferrous and ferric iron. For example, melts produced at pressures of 6.3 and 7.5 GPa in the (Mg,Ca)CO<sub>3</sub>-SiO<sub>2</sub>-Al<sub>2</sub>O<sub>3</sub>-Fe<sup>0</sup> system can contain up to 43 wt.% of iron oxides in the dissolved form and are characterized by Fe<sup>3+</sup>/ΣFe values of ~0.18–0.23 (Bataleva et al., 2015). The melts obtained in the present study are characterized by even higher concentrations of FeO, up to 56 wt.%. Given a high concentration of Fe<sup>3+</sup> and carbonate component in these melts, it may be supposed that their migration throughout the various upper mantle domains can lead to a significant change in the redox potential and mineral/component composition of these domains.

#### 4.3. Implications of interaction processes of wüstite and CO<sub>2</sub>-rich fluid or carbonate-silicate melt in natural deep mantle environments

A number of studies, concerned with the deep carbon cycle (Dasgupta, 2013; Shirey et al., 2013; Walter et al., 2011), demonstrated that subduction is the main mechanism of production and transportation of carbonate-bearing melts and components of C-O-H fluid into the lithospheric mantle. It is shown that subduction of crustal material not only initiates partial melting and generation of aqueous fluids via slab dehydration and decarbonation in the upper mantle (Klein-BenDavid et al., 2009, 2010; Kopylova et al., 2010; Schrauder and Navon, 1994; Walter et al., 2008) but also results in the redox interaction between oxidized slab and relatively reduced deep mantle rocks (Rohrbach and Schmidt, 2011), since the oxidized carbonate-bearing crustal material can be preserved in a slab up to depths of ≥ 600 km (Harte and Richardson, 2012; Shirey et al., 2013; Walter et al., 2011). As evidenced by the compositions of inclusions in diamond, containing carbonates and CO<sub>2</sub>-fluid (Klein-BenDavid et al., 2004; Schrauder and Navon, 1993; Shirey et al., 2013; Sobolev et al., 2009; Stachel et al., 1998; Wang et al., 1996) and thermodynamic data (Boulard et al., 2011; Oganov et al., 2013), some part of carbonates in the subducted rocks can be stable up to *P*-*T* conditions of the lower mantle. According to these data, it is supposed that subducted carbonates can act as a

source of CO<sub>2</sub>-rich fluids and carbonate-bearing melts in a very wide range of pressures and temperatures.

In the present study, we show the results of wüstite + CO<sub>2</sub> and wüstite + carbonate-silicate melt interaction, which can be expected to occur in a course of subduction. Interaction of wüstite-bearing rocks with CO<sub>2</sub>-rich fluid and carbonatitic melts, which are both believed to be mobile oxidizing mantle metasomatic agents, can have a number of consequences. In the presence of strongly oxidized CO<sub>2</sub>-rich fluid or carbonatitic melt, wüstite is unstable; so, depending on *f*O<sub>2</sub>, it can be oxidized to form Fe<sup>3+</sup>-bearing wüstite + graphite or magnetite + graphite assemblages or it can be totally dissolved in a metasomatic agent. The latter results in the formation of Fe<sup>2+</sup>, Fe<sup>3+</sup>-enriched carbonate-bearing melt. According to modern concepts, redox conditions in the mantle conform to very complex patterns. Particularly, there are findings of mantle xenoliths, which underwent intense metasomatic oxidation, with the oxygen fugacity in them reaching FMQ + 1 log unit (Creighton et al., 2009; Woodland and Koch, 2003). The presence of highly oxidized rocks confirm the assumption that some domains of the lithospheric mantle was altered by mobile oxidized metasomatic agents, such as Fe<sup>3+</sup>-bearing silicate melts (Hirschmann, 2009; Kelley and Cottrell, 2009), similar to melts, synthesized in the present work. It was established that interaction of wüstite and carbonate-silicate melt results not only in the enrichment of carbonate-silicate melt with Fe<sup>2+</sup> and Fe<sup>3+</sup>, but also leads to crystallization of fayalite-magnetite spinel solid solution, which is believed to be one of potential Fe<sup>3+</sup>-bearing phases in the Earth's mantle and transition zone (Woodland and Angel, 2000).

#### 4.4. Conditions of the graphite and diamond stability

The formation of metastable graphite and growth of diamond due to the interaction in the FeO-MgO-CaO-SiO<sub>2</sub>-Al<sub>2</sub>O<sub>3</sub>-CO<sub>2</sub> system occur only in relatively low temperature experiments (1150 °C–1250 °C) in the reaction zone at the contact of wüstite with the carbonate-oxide ampoule. Given the fact that the association of wüstite and magnetite forms in the reaction zone, and the amount of a CO<sub>2</sub>-rich fluid formed during decarbonation is very small, the oxygen fugacity value in these sample fragments can be roughly estimated to be close to that of the wüstite-magnetite buffer. In this temperature range, *f*O<sub>2</sub> values characteristic of the wüstite-magnetite (WM) buffer fall within the stability field of elemental carbon. In connection with this, metastable graphite crystallization occurs, and the initial stage of diamond growth on seed crystals is observed. As the main mechanism for graphite formation and diamond crystallization, the partial reduction of CO<sub>2</sub> by magnesiowüstite to elemental carbon and corresponding oxidation of (Fe,Mg)O to Fe<sup>3+</sup>-bearing magnesiowüstite and magnetite via redox interactions (7) and (8) may be considered. Only single metastable graphite crystals as well as the initial stage of dissolution of diamond seed crystals were observed in the experiment at 1350 °C with the presence of the magnetite and magnesiowüstite assemblage and a large amount of decarbonation-derived CO<sub>2</sub>. Analysis of the seed crystal micromorphology revealed that positively oriented etching pits are present on the surface of (111) faces, which indicates the dissolution of diamond in a CO<sub>2</sub>-rich fluid (Khokhryakov and Pal'yanov, 2007). A set of phases produced in the experiment at 1350 °C is a marker of very close *f*O<sub>2</sub> values for the buffer equilibria of CCO and WM. At temperatures ≥ 1450 °C and in the presence of a carbonate-silicate melt, diamond seed crystals had traces of strong dissolution with the patterns characteristic of diamond exposure to oxidized melts of alkaline earth carbonates saturated with a CO<sub>2</sub>-fluid (Khokhryakov and Pal'yanov, 2007). According to our estimations, the sample *f*O<sub>2</sub> values under these conditions are beyond the limits of the elemental carbon stability, between the CCO and WM buffers, while carbonate-silicate melts are characterized by Fe<sup>3+</sup>/ΣFe of about 0.03–0.06. A study (Stagno et al., 2013) demonstrated that under conditions of the lithospheric mantle, at depths of 180–220 km, the generation of carbonate-silicate melts with

$\text{Fe}^{3+}/\Sigma\text{Fe} = 0.06$  occurs at  $f\text{O}_2$  values of about FMQ-1, which is in good agreement with our results.

It is necessary to address particularly the question of experimental modeling of the graphite and diamond formation from carbon of carbonates, which was demonstrated in this study. In the earliest experimental studies where diamond was produced from carbon of carbonates, the reducing agents were silicon and silicon carbide (Arima et al., 2002), hydrogen (Pal'yanov et al., 2002a, 2002b; Pal'yanov et al., 2005), and also silicon and  $\epsilon$ -FeSi (Siebert et al., 2005). In our previous studies concerned with the modeling of diamond formation in nature, we showed that sulfides, iron carbide, and metallic iron can serve as reducing agents for carbonates and a  $\text{CO}_2$ -fluid (Bataleva et al., 2015; Palyanov et al., 2007, 2013). The present study demonstrates the potential role of wüstite/magnesiowüstite as a reductant of  $\text{CO}_2$  to elemental carbon under lithospheric mantle conditions.

## 5. Conclusions

In the course of carbonate–oxide interaction in the FeO–MgO–CaO– $\text{SiO}_2$ – $\text{Al}_2\text{O}_3$ – $\text{CO}_2$  system at pressure of 6.3 GPa and in the range of 1150 °C–1350 °C, decarbonation reactions giving rise to  $\text{CO}_2$ -rich fluid, magnesiowüstite, and iron-rich garnet occur. At these temperatures, magnesiowüstite is able to partially reduce  $\text{CO}_2$  to  $\text{C}^0$  that results in crystallization of magnetite and metastable graphite and initial growth of the diamond phase (1150 °C–1250 °C).

The complete oxidation of magnesiowüstite was found to occur in the temperature range of 1450 °C–1650 °C. At 1450 °C, the first portion of the iron-bearing carbonate–silicate melt was produced. The melt contained ~56 wt.% of iron oxides ( $\text{Fe}^{3+}/\Sigma\text{Fe} \sim 0.06$ ). At 1550 °C–1650 °C, high degrees of melting and decarbonation of the system lead to the generation of the  $\text{Fe}^{2+}$ -rich, carbonate–silicate melt, coexisting with pyrope–almandine  $\pm$  ferromagnesite assemblage. Dissolution (oxidation) of diamond was found to occur in the presence of the carbonate–silicate melt. In this case, the degree of diamond dissolution increases as the concentration of  $\text{CO}_2$ -rich fluid and partial melting degree are increased.

The study results demonstrate that under conditions of the lithospheric mantle, wüstite/magnesiowüstite is stable in the presence of a  $\text{CO}_2$ -rich fluid at relatively low temperatures only when FeO is in an absolute excess relative to  $\text{CO}_2$ . Under these conditions, the formation of graphite and diamond was found to occur due to the wüstite +  $\text{CO}_2$  redox interaction accompanied by oxidation of wüstite to  $(\text{Fe}^{2+}, \text{Fe}^{3+})\text{O}$  and magnetite. At higher temperatures and increased concentrations of a  $\text{CO}_2$ -fluid as well as in the presence of the carbonate–silicate melt, wüstite is unstable. It is completely oxidized to magnetite or dissolves in the melt that leads to the formation of  $\text{Fe}^{2+}$ - and  $\text{Fe}^{3+}$ -enriched carbonate–silicate melts, which are potential metasomatic agents in the lithospheric mantle.

## Acknowledgements

This work was supported by the Russian Science Foundation under grant no. 14-27-00054. The authors thank A. Moskalev for his assistance in the work preparation, A. Khokhryakov for useful suggestions throughout the study, and S. Ovchinnikov for his assistance in implementation of Mössbauer spectroscopy measurements. The authors thank editor M. Scambelluri, and two anonymous reviewers for their useful comments, which helped to profoundly improve the manuscript.

## Appendix A. Supplementary data

Supplementary data to this article can be found online at <http://dx.doi.org/10.1016/j.lithos.2015.12.001>.

## References

- Arima, M., Kozai, Y., Akaishi, M., 2002. Diamond nucleation and growth by reduction of carbonate melts under high-pressure and high-temperature conditions. *Geology* 30, 691–694.
- Bataleva, Y.V., Palyanov, Y.N., Sokol, A.G., Borzdov, Y.M., Palyanova, G.A., 2012a. Conditions for the origin of oxidized carbonate–silicate melts: implications for mantle metasomatism and diamond formation. *Lithos* 128–131, 113–125.
- Bataleva, Y.V., Pal'yanov, Y.N., Sokol, A.G., Borzdov, Y.M., Sobolev, N.V., 2012b. Conditions of formation of Cr–pyrope and escolaitite during mantle metasomatism: Experimental modeling. *Doklady Earth Sciences* 442 (1), 76–80.
- Bataleva, Y.V., Palyanov, Y.N., Sokol, A.G., Borzdov, Y.M., Bayukov, O.A., 2015. The role of rocks saturated with metallic iron in the formation of ferric carbonate–silicate melts: experimental modeling under PT-conditions of lithospheric mantle. *Russian Geology and Geophysics* 56 (1–2), 143–154.
- Berman, R.G., 1991. Thermobarometry using multiequilibrium calculations: a new technique with petrologic applications. *Canadian Mineralogist* 29, 833–855.
- Biellmann, C., Gillet, P., Guyot, F., Peyronneau, J., Reynard, B., 1993. Experimental evidence for carbonate stability in the Earth's lower mantle. *Earth and Planetary Science Letters* 118, 31–41.
- Boulard, E., Gloter, A., Corgne, A., Antonangeli, D., Auzende, A.-L., Perrillat, J.-P., Guyot, F., Fiquet, J., 2011. New host for carbon in the deep Earth. *Proceedings of the National Academy of Sciences of the United States of America* 108 (13), 5184–5187.
- Brenker, F.E., Vollmer, C., Vincze, L., Vekemans, B., Szymanska, A., Janssens, K., Szaloki, I., Nasdala, L., Joswig, W., Kaminsky, F., 2007. Carbonates from the lower part of transition zone or even the lower mantle. *Earth and Planetary Science Letters* 260 (1–2), 1–9.
- Bulanova, G.P., 1995. The formation of diamond. *Journal of Geochemical Exploration* 53, 2–23.
- Creighton, S., Stachel, T., Matveev, S., Höfer, H., McCammon, C., Luth, R.W., 2009. Oxidation of the Kaapvaal lithospheric mantle driven by metasomatism. *Contributions to Mineralogy and Petrology* 157, 491–504.
- Dasgupta, R., 2013. Ingassing, storage, and outgassing of terrestrial carbon through geologic time. *Reviews in Mineralogy and Geochemistry* 75, 183–229.
- Dubrovinsky, L.S., Dubrovinskaya, N.A., Annersten, H., Hälenius, E., Harryson, H., Tutti, F., Rekh, S., LeBihan, T., 2000. Stability of ferropericlase in the lower mantle. *Science* 289, 430–432.
- Fei, Y., Mao, H.K., Shu, J., Hu, J., 1992. P–V–T equation of state of magnesiowüstite ( $\text{Mg}_{0.6}\text{Fe}_{0.4}\text{O}$ ). *Physics and Chemistry of Minerals* 18, 416–422.
- Finger, L.W., 1972. The Uncertainty in Calculated Ferric Iron Content of a Microprobe Analysis? 71. *Carnegie Institute Washington, Yearbook*, pp. 600–603.
- Frost, D.J., McCammon, C.A., 2008. The redox state of Earth's mantle. *Annual Review of Earth and Planetary Sciences* 36, 389–420.
- Harte, B., 2010. Diamond formation in the deep mantle: the record of mineral inclusions and their distribution in relation to mantle dehydration zones. *Mineralogical Magazine* 74 (2), 189–215.
- Harte, B., Hudson, N.F.C., 2013. Mineral associations in diamonds from the lowermost upper mantle and uppermost lower mantle. *Proceedings of the 10th International Kimberlite Conference. Geological Society of India* vol. 1, pp. 235–253.
- Harte, B., Richardson, S., 2012. Mineral inclusions in diamonds track the evolution of a Mesozoic subducted slab beneath West Gondwanaland. *Gondwana Research* 21 (1), 236–245.
- Harte, B., Harris, J.W., Hutchison, M.T., Watt, G.R., Wilding, M.C., 1999. Lower mantle mineral associations in diamonds from São-Luiz, Brazil. In: Fei, Y., Bertka, C.M., Mysen, B.O. (Eds.), *Mantle petrology: field observations and high pressure experimentation; a tribute to Francis R. (Joe) Boyd*: Geochemical Society Special Publication, No 6, pp. 125–153.
- Hayman, P.C., Kopylova, M.G., Kaminsky, F.Y., 2005. Lower mantle diamonds from Rio Soriso (Juina area, Mato Grosso, Brazil). *Contributions to Mineralogy and Petrology* 149, 430–445.
- Hirschmann, M.M., 2009. Ironing out the oxidation of Earth's mantle. *Science* 325 (5940), 545–546.
- Kaminsky, F., 2012. Mineralogy of the lower mantle: A review of 'super-deep' mineral inclusions in diamond. *Earth-Science Reviews* 110 (1–4), 127–147.
- Kaminsky, F.V., Wirth, R., Schreiber, A., 2013. Carbonatic inclusions in deep mantle diamond from Juina, Brazil: new minerals in the carbonate–halide association. *Canadian Mineralogist* 51 (5), 447–466.
- Kaminsky, F.V., Ryabchikov, I.D., McCammon, C.A., Longo, M., Abakumov, A.M., Turner, S., Heidari, H., 2015. Oxidation potential in the Earth's lower mantle as recorded by ferropericlase inclusions in diamond. *Earth and Planetary Science Letters* 417, 49–56.
- Kelley, K.A., Cottrell, E., 2009. Water and the oxidation state of subduction zone magmas. *Science* 325 (5940), 605–607.
- Khokhryakov, A.F., Pal'yanov, Y.N., 2007. The evolution of diamond morphology in the process of dissolution: experimental data. *American Mineralogist* 92, 909–917.
- Klein-BenDavid, O., Israeli, E.S., Hauri, E., Navon, O., 2004. Mantle fluid evolution: a tale of one diamond. *Lithos* 77 (1–4), 243–253.
- Klein-BenDavid, O., Logvinova, A.M., Schrauder, M., Spetius, Z.V., Weiss, Y., Hauri, E.H., Kaminsky, F.V., Sobolev, N.V., Navon, O., 2009. High-Mg carbonatic microinclusions in some Yakutian diamonds: a new type of diamond-forming fluid. *Lithos* 112, 648–659.
- Klein-BenDavid, O., Pearson, D.G., Nowell, G.M., Ottley, C., McNeill, J.C.R., Cartigny, P., 2010. Mixed fluid sources involved in diamond growth constrained by Sr–Nd–Pb–C–N isotopes and trace elements. *Earth and Planetary Science Letters* 289, 123–133.
- Knoche, R., Sweeney, R.J., Luth, R.W., 1999. Carbonation and decarbonation of eclogites: the role of garnet. *Contributions to Mineralogy and Petrology* 135, 332–339.
- Kopylova, M., Navon, O., Dubrovinsky, L., Khachatryan, G., 2010. Carbonatic mineralogy of natural diamond-forming fluids. *Earth and Planetary Science Letters* 291, 126–137.

